Ultrafast Fluorescence Relaxation Spectroscopy of 6,7-Dimethyl-(8-ribityl)-lumazine and Riboflavin, Free and Bound to Antenna Proteins from Bioluminescent Bacteria

Valentin N. Petushkov,[†,‡] Ivo H. M. van Stokkum,[§] Bas Gobets,[§] Frank van Mourik,[§,#] John Lee,[⊥] Rienk van Grondelle,[§] and Antonie J. W. G. Visser*[,†,▽]

MicroSpectroscopy Centre, Laboratory of Biochemistry, Wageningen University, Dreijenlaan 3, 6703 HA Wageningen, The Netherlands, Department of Physics and Astronomy, Faculty of Sciences, Vrije Universiteit, De Boelelaan 1081, 1081 HV Amsterdam, The Netherlands, Department of Biochemistry and Molecular Biology, University of Georgia, Athens, Georgia 30602, and Department of Structural Biology, Faculty of Earth and Life Sciences, Vrije Universiteit, De Boelelaan 1087, 1081 HV Amsterdam, The Netherlands

Received: January 31, 2003; In Final Form: April 14, 2003

The solvation dynamics of interesting bioluminescent chromophores have been determined, using subpicosecond and wavelength-resolved fluorescence spectroscopy, in combination with global analysis of the multidimensional data sets. The systems investigated comprise the free ligands 6,7-dimethyl-(8-ribityl)-lumazine (lumazine) and riboflavin in an aqueous buffer and both ligands when noncovalently bound to two bacterial bioluminescent antenna proteins: lumazine protein (from *Photobacterium leiognathi*) and the blue fluorescent protein (from *Vibrio fischeri* Y1). Fluorescence spectral relaxation of the free ligands is complete within a few picoseconds. Subsequently, the fluorescence intensity increases by ∼7% on a time scale of 15−30 ps. Fluorescence spectral relaxation of the protein-bound ligands is largely complete within 1 ps but reveals a small red shift with a minor, but distinctly longer, relaxation time than that of the free ligands, which is tentatively assigned to the relaxation of protein-bound water in the vicinity of the excited chromophore.

Introduction

The exact location of the fluorescence spectral maximum of a fluorescent molecule is dependent on the dielectric properties of the medium in which the fluorophore resides. Generally, because of the thermal motions of solvent molecules, the chromophore will exhibit a stochastic deviation of the dipolar interaction energies, resulting in a distribution of singlet−singlet transition frequencies and an inhomogeneous spectral broadening by fluctuating chromophore−solvent interactions.[1−7] The technique of fluorescence relaxation spectroscopy is aimed at following such spectral changes with time. Of particular interest is the application of fluorescence relaxation spectroscopy to proteins, where the solvent is water that forms a hydration shell around the protein globule. The protein-bound water is in rapid dynamic equilibrium with free water, which is characterized by dielectric relaxation times in the picosecond and nanosecond time regime.[8] Tryptophan residues are widely used as intrinsic fluorescent markers for studying solvation dynamics both experimentally and theoretically (for recent applications, see refs 9−14). In other recent reports, extrinsic fluorescent probes have been exploited, such as eosin bound to lysozyme,[15] a coumarin that contained peptide bound to calmodulin,[16] a dansyl chromophore covalently linked to subtilisin,[12] and an alanine derivative of 6-(dimethylamino)-2-acyl-naphthalene that was introduced as a fluorescent amino acid in protein G.[17] Very recently, a theoretical description of protein hydration has been developed and compared to experimental observations.[18]

Another class of intrinsically fluorescent proteins used to examine solvation dynamics are the flavoproteins. The flavin in this case can be considered as a natural fluorescent reporter group that can probe the dynamical structure of the active site of flavoproteins. Earlier steady-state fluorescence studies were performed to obtain information on the dynamical properties of the direct environment of the flavin of the prosthetic group flavin adenine dinucleotide (FAD).[19−21] Somewhat later, picosecond-timescale and wavelength-resolved fluorescence spectroscopy were applied to follow these dipolar relaxation processes in the vicinity of flavins directly, even in nonviscous media.[22] When the fluorescence of a model flavin in ethanol is detected in the blue portion of the emission band, a rapid decay component can be observed. Upon detection at the red portion of the flavin fluorescence band, an increase in intensity can be observed. This behavior is consistent with a gradual spectral red shift during solvation. However, the solvation dynamics of a free flavin, such as in flavin mononucleotide (FMN) in water, was shown to be so rapid that the time resolution of the measuring system (>5 ps with a 4-ps laser-pulse excitation and detection with time-correlated single photon counting) is not sufficient to register the complete effect.[23] For the study of ultrarapid solvation, one must rely on an experimental system with femtosecond resolution, such as one that consists of a subpicosecond laser as the excitation source and a polychromator and synchroscan streak camera in the detection channel. This system is very appropriate for studying dipolar relaxation of biological fluorophores, because the emission can be measured

* Author to whom correspondence should be addressed. E-mail: Ton.Visser@wur.nl.
[†] Wageningen University.
[‡] Permanent address: Institute of Biophysics, Academy of Sciences of Russia, Krasnoyarsk 660036, Russia.
[§] Department of Physics and Astronomy, Faculty of Sciences, Vrije Universiteit.
[#] Current address: Institut de Physique de la Matière Condensée (IPMC), BSP, Université de Lausanne, CH 1015 Lausanne, Switzerland.
[⊥] University of Georgia.
[▽] Department of Structural Biology, Faculty of Earth and Life Sciences, Vrije Universiteit.

10.1021/jp034266e CCC: $25.00
Published on Web 08/28/2003

CHART 1

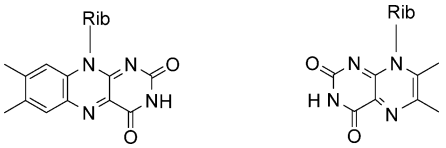

across three dimensions (time, wavelength (energy), and intensity) in a single experiment. These multidimensional data sets can then be analyzed globally to recover the relaxation time(s). Experiments using this system and associated data analysis will be described in this paper. This setup was recently used to measure ultrarapid flavin fluorescence of FAD in a mutant of thioredoxin reductase.[24]

Using the latter approach, the natural fluorescence of the antenna proteins that are derived from the bioluminescent bacteria serves as a good example for the investigation of ultrafast fluorescence relaxation spectroscopy of the protein-bound fluorophores and allows the results obtained to be compared with those of the unbound fluorophores in aqueous solution. These antenna proteins change the color of bioluminescence by the process of resonance energy transfer from the chemically excited bacterial luciferase product (a bound 4a-hydroxyflavin) to the luciferase-associated antenna protein.[25−27] These light-emitting antenna proteins have high fluorescence quantum yields, which facilitate ultrafast time-resolved fluorescence experiments. Moreover, their relatively long fluorescence lifetime allows for dynamic studies over a time window of several nanoseconds. Two proteins are used in this study: the lumazine protein (LumP) from *Photobacterium leiognathi*[28,29] and the so-called blue-fluorescent protein (Lum-BFP), which is isolated from yellow bioluminescence bacteria (*Vibrio fischeri* strain Y1).[30] Both proteins have noncovalently bound 6,7-dimethyl-(8-ribityl)-lumazine (hereafter abbreviated simply as lumazine) as a prosthetic group. Both riboflavin and lumazine are structurally related (riboflavin, on the lefthand side of Chart 1, contains an extra benzene ring that is fused to the pyrimidine portion of lumazine, which is shown on the righthand side of Chart 1); therefore, lumazine can be replaced by riboflavin in both proteins (abbreviated as Rf-LumP and Rf-BFP, respectively). Rf-LumP and Rf-BFP are highly fluorescent flavoproteins in which the binding site is optimized for maximum quantum yield of flavin emission.[31,32]

Materials and Methods

Materials, Steady-State Spectroscopy, and Sample Preparation. Lumazine was supplied as a gift from Professor A. Bacher (Munich Technical University, Garching, Germany). The proteins were purified according to protocols that have been described previously.[29,31] The proteins were dissolved in a 25 mM sodium phosphate buffer (pH 7). Concentrations for free lumazine and riboflavin in water were determined from the light absorption at 408 and 445 nm, using molar extinction coefficients of 10 300 and 12 500 M^{-1} cm^{-1}, respectively. For proteins with bound lumazine, a molar extinction coefficient of 10 100 M^{-1} cm^{-1} (LumP at 420 nm and Lum-BFP at 417 nm) was used for concentration determinations. For proteins that were reconstituted with riboflavin, concentrations were measured using a molar extinction coefficient of 12 500 M^{-1} cm^{-1} (Rf-LumP at 463 nm and Rf-BFP at 457 nm). The lumazine ligand on LumP and Lum-BFP was exchanged by riboflavin, using a protocol that was extensively detailed elsewhere.[33] Steady-state absorption and fluorescence spectra were obtained as described previously.[33] For the ultrafast fluorescence measurements (vide infra), the concentrations used for the free ligands were ∼100 μM. The concentrations of the bound ligands were 40 μM for Lum-BFP, 42 μM for LumP, 22 μM for Rf-BFP, and 95 μM for Rf-LumP.

Time-Resolved Fluorescence Data Collection and Preprocessing. For the excitation of the sample, the frequency-doubled light from a Mira RegA (Coherent) oscillator/regenerative amplifier combination was used, giving pulses of ∼200 fs full width at half-maximum (fwhm), at a repetition rate of 50−125 kHz. The pulse was centered at 400 nm and possessed a spectral width of 10 nm fwhm. The pulse energy was 20−40 nJ. The protein samples were more dilute than the free ligands; thus, longer integration times and more averaging were necessary. The pulses were focused into the sample, using an $f = 15$ cm lens. The protein sample was contained in a rotating cell (ca. 300 rpm) to prevent excessive accumulation effects. Under the experimental conditions, each spot is hit by <10 pulses per transit through the focus. The light path of the cell was 3 mm, and the (horizontal) focus of the laser was imaged onto the (vertical) slit of the spectrograph, using *f*/8 optics. The isolated chromophore samples were contained in a flow cell (using a flow rate of 1 mL/s). The synchroscan streak camera (Hamamatsu models C5680 and M5675) was synchronized to the Mira oscillator, using a photodiode (Hamamatsu C1808-02). The fwhm of the instrument response function (IRF) of the streak camera without a spectrograph was typically 1.8 ps. The IRF of the total system including the Chromex model IS250 spectrograph, which was equipped with a 50 grooves/mm grating, was 2.6−3.5 ps; this value was checked using white-light continuum pulses that were generated by focusing the RegA output in a 2-mm sapphire plate to simulate a broadband emission spectrum. Measurements were performed with the help of a data acquisition system that included a model C4880 Dual Scan cooled CCD camera (Hamamatsu model HPD TA). Accumulations of up to 600 s per data set (accumulation on the CCD chip) resulted in an image of the fluorescence intensity as a function of time and wavelength. Up to eight images were averaged. The full time and wavelength ranges were 200 ps and 300 nm, respectively. Data were corrected for dark current and shading.[34] A crucial procedure for the analysis of the two-dimensional data sets is the characterization of the curvature of the image. The image of the entrance slit of the streak camera on the CCD camera is curved, because of the spatial dependence of the time-zero point of the image. In addition, of course, the light-collecting optics and the spectrograph also cause wavelength-dependent temporal shifts. Thus, the dispersion of the white-light pulse used for this calibration was measured using the optical Kerr signal in carbon disulfide.[35]

The wavelength resolution of the monochromator was ∼8 nm; therefore, the curvature-corrected and averaged images were reduced to a matrix of 1000 points in time and 33 points in wavelength.

Excitation was polarized horizontally, whereas detection was polarized vertically with the proteins. With the isolated chromophores, detection was conducted at the magic angle. All experiments were conducted at a temperature of 295 K.

Data Analysis. First, we derive the expression used to describe the contribution of an exponentially decaying component to the streak image, corrected for the instrumental curvature. The instrument response $i(t)$ was adequately modeled with a Gaussian with parameters for location μ and width τ:

$$i(t) = \frac{1}{\sqrt{2\pi\tau^2}} e^{-(t-\mu)^2/(2\tau^2)} \quad (1)$$

The width of $i(t)$ (and, thus, the temporal resolution) is limited by the point-spread function of the imaging device and by the temporal spread that results from the monochromator. When using the fastest time base of 200 ps, the width of $i(t)$ is typically 3 ps fwhm (which corresponds to 15 pixels on the CCD).

The convolution (which is indicated by an asterisk, *) of this instrument response with an exponential decay results in an analytical expression that facilitates the estimation of the instrument response parameters μ and τ:[36]

$$e^{-kt} * i(t) = \frac{e^{-kt}}{2} e^{-k(\mu+k\tau^2/2)} \left\{1 + \mathrm{erf}\left[\frac{t-(\mu+k\tau^2)}{\sqrt{2}\tau}\right]\right\} \quad (2)$$

The periodicity of the synchroscan results in detection of the remaining fluorescence after multiples of half the period T of 13.4 ns. Thus, for lifetimes of >1 ns, a sum of exponential decays that result from forward and backward sweeps must be added to the aforementioned expression:

$$\sum_{n=0}^{\infty} e^{-kTn}\{e^{-k(t-\mu+T)} + e^{-k(T/2-t-\mu)}\} = \frac{e^{-k(t-\mu+T)} + e^{-k(T/2-t-\mu)}}{1 - e^{-kT}} \quad (3)$$

With the relatively dilute samples, the Raman scattering of water (centered at ~467 nm) complicated the measurement. We modeled it as an extra component that contributed only between 450 and 480 nm, with a time course that was identical to the instrument response.

Below, we will consider two types of compartmental models: (1) a model with components that are decaying in parallel, which results in decay-associated spectra (DAS), and (2) a sequential model with increasing lifetimes, also called unbranched unidirectional model, giving species-associated spectra (SAS). The first SAS (equal to the sum of the DAS) corresponds to the spectrum at time zero with an ideal $i(t) = \delta(t)$. The final SAS is equal to the final DAS and represents the spectrum of the longest-living component. In turn, the SAS are fitted with a spectral model, for which we take a skewed Gaussian in the energy domain ($\bar{\nu} = 1/\lambda$):[36]

$$\mathrm{SAS}(\bar{\nu}) = \bar{\nu}^5 S_{\max} \exp\left(-\ln(2)\left\{\ln\left[\frac{1 + 2b(\bar{\nu} - \bar{\nu}_{\max})}{\Delta\bar{\nu}}\right]/b\right\}^2\right) \quad (4)$$

where $\bar{\nu}_{\max}$ is the Franck−Condon wavenumber of maximum emission. The fwhm is given by $\Delta\bar{\nu}_{1/2} = \Delta\bar{\nu}\ (\sinh b)/b$. Note that eq 4 simplifies to a Gaussian with the skewness parameter b equal to zero.

Results

Steady-State Absorption and Fluorescence Spectra. Typical normalized absorption spectra and steady-state fluorescence spectra of free and bound ligands[33] are shown in Figure 1. The fluorescence spectra have been fitted using eq 4, and the results are shown in Figure S.1 in the Supporting Information. Light absorption maxima—and fluorescence emission maxima, fwhm, and nanosecond lifetimes[37]—for free and protein-bound lumazine and riboflavin are collated in Table 1. The light absorption maxima in the visible and near-UV region of free riboflavin are blue-shifted by ~10 nm, in comparison to bound riboflavin. This negative solvatochromism will be discussed below (see Discussion). The fluorescence maxima of free riboflavin and Rf-LumP are almost the same, whereas that of Rf-BFP is blue-shifted by ~10 nm. The visible absorption maximum of free lumazine is also blue-shifted by ~10 nm, in comparison to bound lumazine, whereas the emission maximum of free lumazine is distinctly red-shifted by ~20 nm. Both absorption and fluorescence spectra of the bound ligands show a characteristic vibrational fine structure.[33] This is illustrated by the residuals shown in the insets of Figure S.1 of the Supporting Information. The fine structure of these residuals corresponds to a periodicity of 1800 ± 400 cm^{-1}. These distinct vibronic shoulders are hardly visible in the spectra of unbound lumazine and riboflavin. Furthermore, the spectral widths of the free ligands are broader than those of the protein-bound ligands (Table 1). Such an effect is indicative of increased inhomogeneous spectral broadening of the free fluorophores, because of the completely relaxed surroundings of water molecules, whereas the bound fluorophores are located in a more constrained environment and are only in partial contact with water. As judged from the different spectroscopic properties of the three lumazine and three riboflavin samples, there are at least three different microenvironments for lumazine and riboflavin, and we can conclude that the ligands in the protein matrix sense a more hydrophobic and constrained surroundings, in agreement with a smaller Stokes shift.

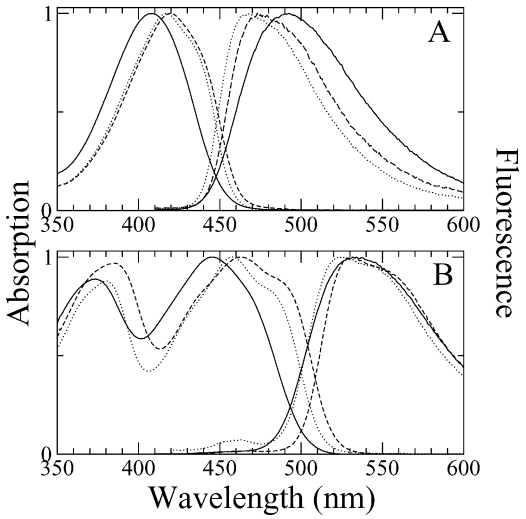

Figure 1. Peak-normalized absorption spectra and fluorescence emission spectra (λ_{exc} = 400 nm) measured in aqueous buffer solution; the emission spectra have not been corrected for the instrument response.[33] Panel A shows data for lumazine (free lumazine is denoted by the solid lines, and lumazine bound to antenna proteins in represented by dashed lines (LumP) and dotted lines (Lum-BFP)), whereas panel B shows data for riboflavin (free riboflavin is denoted by the solid lines, and riboflavin bound to antenna proteins is represented by the dashed lines (Rf-LumP) and dotted lines (Rf-BFP)).

TABLE 1: Spectroscopic Properties of Lumazine and Riboflavin, Free and Bound to Antenna Proteins[a]

sample	absorbance maxima (nm)[a]	fluorescence maximum (nm)[a]	fluorescence fwhm (cm^{-1})	fluorescence lifetime (ns)[b]
lumazine	408	492	4100	10.0
Lum-BFP	417	467	3800	13.4
LumP	420	473	3600	15.3
riboflavin	373, 445	534	3700	4.9
Rf-BFP	381, 457	523	3500	5.7
Rf-LumP	386, 463	531	3600	6.0

[a] From Petushkov et al.[33] [b] From Petushkov and Lee.[37]

Time- and Wavelength-Resolved Fluorescence Emission. In the global analysis of the lumazine and riboflavin aqueous

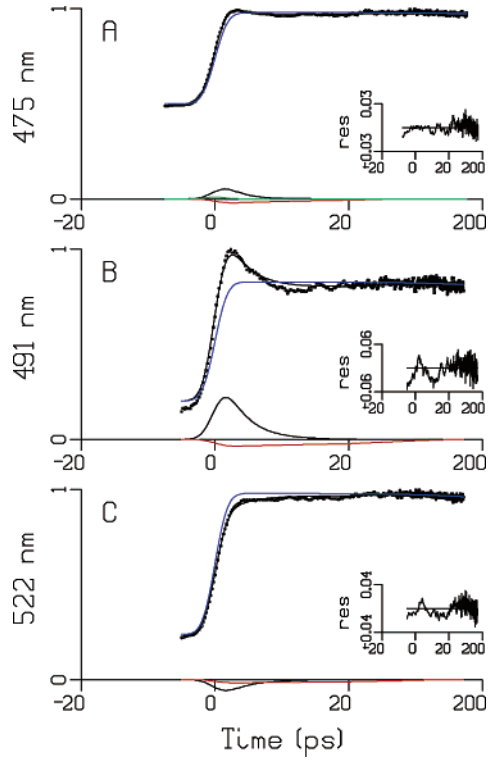

Figure 2. Results from the global analysis of (normalized) kinetics in (A) lumazine and (B and C) riboflavin at representative wavelengths; the insets show residuals of a fit with three exponential decays. The contributions of these decays to the fit are depicted by different colors. Key: 2.7 ps (black in A), 15 ps (red in A), 10 ns (blue in A), 3.5 ps (black in B,C), 36 ps (red in B,C), 4.7 ns (blue in B,C), Raman scattering (green in A). The sum of these contributions is also represented by a solid black line through the measuring points. The time base from −20 ps to +20 ps (relative to the maximum of the instrument response) is linear, and that from 20 ps to 200 ps is logarithmic.

solution data, three exponentially decaying components were needed. Traces at indicated emission wavelengths are shown in Figure 2 (lumazine in Figure 2A; riboflavin in Figure 2B,C). The signal before time zero is due to the periodicity of the synchroscan, in combination with the long lifetime (see previous discussion in text). From the relative magnitude of this signal, the nanosecond lifetime can be estimated (see eq 3). A fast decay in the period of 0.5−4 ps is clearly visible in Figure 2B, with a smaller contribution in the other samples. The fastest component is represented by the black lines, the next slower (∼10 ps) by the red lines, and the fluorescence lifetime (4.7 ns in the case of riboflavin) by the blue lines. The exact relaxation times and lifetimes are given in the legend to Figure 2 and Table 2.

The protein data all require three exponentials. A fast decay with a time constant in the picosecond range and a minor component with lifetimes of 15−57 ps can be distinguished. Third, the slow fluorescence decay (4.7−17 ns) dominates the signal.

In Figure 3A, the first DAS for free lumazine (the black line) represents the signature of a spectral red shift. The standard errors of the spectra were small, except for the first DAS (black). The estimated relative error of the sub-picosecond lifetimes and corresponding DAS is 30%. When we apply the sequential model (with increasing lifetimes), we find the SAS that is depicted in Figure 3D. The SAS could well be fitted using a skewed Gaussian band shape in every case. For lumazine, the wavenumber of maximum emission red-shifts by 610 cm^{-1}.

TABLE 2: Relaxation Times, Dynamic Stokes Shift, and Fluorescence Lifetimes of Lumazine and Riboflavin, Free and Bound to Antenna Proteins[a]

sample	relaxation time (ps) short	relaxation time (ps) long	dynamic Stokes shift (cm^{-1})	fluorescence lifetime (ns)
		Lumazine		
lumazine	2.7	15	610	10
Lum-BFP	0.6	44	650	13
LumP	0.7	24	450	17
		Riboflavin		
riboflavin	3.5	36	240	4.7
Rf-BFP[b]	0.5	57		5.2
Rf-LumP[b]	1.0	54		5.8

[a] Estimated relative errors are 10%, except for the sub-picosecond lifetimes, which are 30%. [b] Preparation was contaminated with lumazine.

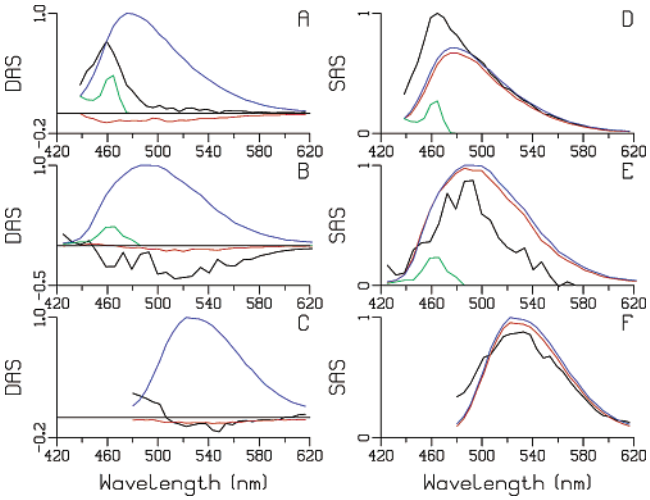

Figure 3. (A−C) Decay associated spectra (DAS) and (D−F) species-associated spectra (SAS) of lumazine (panels A and D), *P. leiognathi* LumP (panels B and E), and riboflavin (panels C and F). Different DAS and SAS are depicted by different colors. Key: 2.7 ps (black in A,D), 15 ps (red in A,D), 10 ns (blue in A,D), 0.7 ps (black in B,E), 24 ps (red in B,E), 17 ns (blue in B,E), 3.5 ps (black in C,F), 36 ps (red in C,F), 4.7 ns (blue in C,F), and Raman scattering (green).

With lumazine protein (LumP), the situation is more complicated (Figure 3B,E). First, because of the relatively dilute sample, Raman scattering is present (denoted as the green line in Figure 3). Second, the extra lifetime of 24 ps shows a very small DAS. When applying the sequential model with three components, we forced the first SAS to be zero at >580 nm, because, otherwise, small negative amplitudes resulted. The SAS then seem realistic. The wavenumber of maximum emission red-shifts by 360 cm^{-1} in 0.7 ps, followed by a minor red shift of 90 cm^{-1} in 24 ps. Summarizing, with both lumazine and lumazine protein, we find a dynamic red shift of 610 and 360 cm^{-1}, respectively, in ca. 1 ps. In addition, a further small red shift is present in lumazine protein on a time scale of tens of picoseconds.

All protein−chromophore complexes and free chromophores listed in Table 1 were studied using this procedure. The estimated relaxation times, lifetimes, and complete spectral shifts are summarized in Table 2. The SAS for Lum-BFP, Rf-BFP, and Rf-LumP qualitatively resembled the red shifts illustrated in Figure 3D−F. Quantitatively, with Lum-BFP, the red shifts were 560 cm^{-1} (subpicosecond) and 90 cm^{-1} (44 ps).

In the case of Rf-LumP and Rf-BFP, the recharging with riboflavin was incomplete (also see the small emission at <480 nm in Figure 1B). Therefore, two long lifetimes were needed:

5.8 ns for the Rf-LumP (5.2 ns for Rf-BFP) and 17 ns for the unsubstituted LumP (13 ns for Lum-BFP). The latter possessed only a very small DAS with a shape resembling the 17-ns DAS from Figure 3B. The SAS of Rf-LumP and Rf-BFP did not allow quantitative conclusions on the red shifts.

Discussion

By far, most of the spectral dynamics occur during the first picosecond. The exact time scale on which the time-dependent Stokes shift occurs is difficult to determine accurately. However, the magnitude of the subpicosecond shift is obtained from the analysis with great confidence. The very small amplitude of any spectral shifts that occur on longer time scales (on the edge of what can be determined accurately) suggests that (i) most of the spectral dynamics are due to solvent shifts and (ii) the short time scale involved is a strong indication that the chromophores in both proteins are exposed to water. The DAS of the free ligands (see Figure 3A,C) can be interpreted as an initially blue-shifted spectrum that shifts to the red. Such interpretation is in agreement with a general picture of solvation proposed by others (see, for instance, the work of Pal et al.[18]).

Although the contribution of the Raman scattering and the subpicosecond dynamic Stokes shift both occur well within our instrumental time response, clearly the combination of two-dimensional data with a good correction (no adjustable parameters) for the curvature of the time−wavelength matrix and the spectral restriction of the Raman scattering allows us to distinguish both events with great confidence.

The observed negative solvatochromism is generally an indication that the molecule has a larger dipole moment in the ground state than in the excited state.[38] This situation is not so strange, considering that the dipole moment calculated for the flavin ground state totals ~7 D,[39] whereas the experimental S_1 dipole moment is only slightly larger (by ~1 D).[20] The calculated value obviously pertains to the unsolvated (gas-phase) flavin molecule; in a dielectric medium, it is very likely that the actual dipole moment of the molecule in the ground state is enhanced. This would be caused by the reaction field that is induced by the dipole moment in the solvent, which, in turn, further polarizes the ground-state molecule (which enhances the dipole moment). The additional polarization of the molecule is normally accompanied by a decrease of the dipole strength of the transition.[40] We actually think that the observed increase of the fluorescence intensity that we observe on a picosecond timescale could be due to this effect. The excited state begins (in the Franck−Condon region) with the reaction field of the ground state; therefore, the initially produced excited state, similar to the ground state, has a reduced dipole strength. Because the excited-state dipole moment is similar, solvent reorganization will result in a reduction of the cavity field, which would cause an increase of the dipole strength of the emitting transition. To our knowledge, this would be the first time-resolved change in dipole strength due to solvation. The effect is more easily observed here, because an increase in intensity is striking, whereas the more-normal decrease in intensity that would accompany positive solvatochromism would be difficult to distinguish from other decay processes. Note, however, that the effect generally should occur. Time-resolved Stark spectroscopy would be a suitable technique to prove the role of the electric fields here, as outlined by van Mourik et al.[41] Although the chromophore at hand is rather complex (because it can occur in different redox and/or protonation states[42]), we do not think that these complications have a role in the experiments reported here.

No three-dimensional structures of antenna proteins are yet available; therefore, it is not known how exactly the lumazine and/or riboflavin are bound to these proteins. Because lumazine and riboflavin share the pyrimidine part, it is obvious that this portion forms the primary binding site of the protein. The relaxation times observed in the proteins (Table 2) range from a fraction of a picosecond to tens of picoseconds (20−60 ps). For the protein-bound ligands, the largest portion of the Stokes shift is complete within 1 ps (similar to that of the free ligands). In the case of protein-bound fluorophores, additional small red shifts are occurring over tens of picoseconds. A similar observation was made for the single, exposed tryptophan in the protein subtilisin and for dansylated subtilisin.[12]

Transient absorption spectra of a resorufin dye in (anhydrous) polar solvents indicated that the lifetime of solute−solvent hydrogen bonds totaled a few picoseconds.[43] Molecular dynamics simulations also show evidence of hydrogen bonding of a polar solvent to a dye molecule in its excited state.[44] Both lumazine and riboflavin have a rather polar character, both in the ground state and in the excited state, and both compounds possess heteroatoms in the ring system, which participate in hydrogen bonding.[45,46] Recently, van den Berg et al.[23] performed molecular dynamics simulations of FAD in water, both in the ground and excited state of the flavin. It was observed that, occasionally, a hydrogen-bonded water bridge between the two aromatic rings was formed during the simulation. Direct interaction between water molecules and the excited lumazine or riboflavin may then have a role during the solvent relaxation process.

The presence of the subpicosecond relaxation time, in the case of proteins, suggests that the bound fluorophore is exposed to water. The exposure of bound ligands (both lumazine and riboflavin) to water in the *P. leiognathi* antenna protein has indeed been shown via potassium iodide quenching experiments.[28] The longer dipolar relaxation time (albeit of low amplitude) must be ascribed to the interaction of the fluorophore with bound-water and vicinal amino acid dipoles, which require a longer time to equilibrate after excitation. The two long relaxation times for lumazine bound in two proteins (Table 2) indicate that the binding site in both proteins must be different; this theory is supported by differences in the absorption and fluorescence emission spectra and fluorescence lifetimes (Table 1). The dynamic Stokes shift (which occurs within ~1 ps) that leads to a completely relaxed excited state is ~600 cm^{-1} for free and protein-bound lumazine. This Stokes shift is of similar magnitude as that found from the temperature-dependent fluorescence spectroscopy of free FAD and a flavin model compound in viscous solvents.[19,20]

The emission shift is usually analyzed in terms of a solvation time-correlation function (see, for instance, the work of Maroncelli and co-workers[5,47]):

$$C(t) = \frac{\bar{\nu}(t) - \bar{\nu}(0)}{\bar{\nu}(0) - \bar{\nu}(\infty)} \tag{5}$$

where $\bar{\nu}(t)$, $\bar{\nu}(0)$, and $\bar{\nu}(\infty)$ are the fluorescence frequencies at time t, time zero, and infinity, respectively. Dielectric continuum models predict that, for a single Debye dielectric relaxation time (τ_D), $C(t)$ will decay exponentially with the solvent longitudinal relaxation time:

$$\tau_L = \left(\frac{\epsilon_\infty}{\epsilon_0}\right)\tau_D \tag{6}$$

where ϵ_0 and ϵ_∞ are the static and infinite frequency dielectric

constants, respectively. In polar solvents, τ_L can be much less than τ_D. For water at 298 K, these values are $\tau_L = 0.54$ ps and $\tau_D = 5.16$ ps.[5] However, it was found that solvation is often nonexponential in time.[47−51] Computer simulations have shown that the response of a solvent to a solute in the excited singlet state leads to strongly bimodal results with an ultrafast response that is due to librational motion of solvent molecules and a slower phase that is due to solvent diffusion processes.[52] Both computer simulation and experiment show that water is the fastest relaxing solvent.[49,52] The water response to an excited laser dye shows an ultrafast inertial component (<55 fs) that accounts for approximately half of the total solvent relaxation.[49,52] The remainder occurs more slowly, on the time scale of picoseconds. In the experiments described here, the time resolution is not sufficient to reveal these ultrarapid events.

In conclusion, the results have shown that solvation dynamics of fluorophores in proteins exhibit, in addition to a fast component of 1 ps, a minor but distinct contribution of a longer relaxation time (20−60 ps). These results are in very good agreement with the results of protein hydration that have been reviewed by Pal et al.[18] For two different single-tryptophan proteins, these authors also observed a "bimodal" decay of the hydration correlation function (which decays due to translational and rotational motions of water). An ultrafast relaxation time of typically ≤1 ps was observed, as well as a longer one (typically in the range 15−40 ps). For tryptophan alone, it was observed that hydration was complete within 1 ps. Both relaxation times are related to the residence time of water molecules at the protein surface and are dependent on the binding energies. The short relaxation time is attributed to quasi-free water molecules at the protein surface, whereas the longer relaxation time reflects surface-bound water with binding energies of a few kilocalories per mole. The experimental approach described here would be particularly useful for proteins that have fluorescent markers that are buried further in the protein matrix, because spectral relaxation is slower and more easily measurable.

Acknowledgment. V. N. Petushkov was supported by a fellowship from The Netherlands Organization for Scientific Research (NWO). The investigations were supported by the Council for Earth and Life Sciences (ALW) of NWO.

Supporting Information Available: Fluorescence spectra fitted using eq 4 (PDF). This material is available free of charge via the Internet at http://pubs.acs.org.

Note Added after ASAP Posting. This article was released ASAP on 8/28/2003 before all author corrections had been submitted. The primary changes involved eq 3. The corrected manuscript was posted 9/3/2003. Additional changes to eq 3 were made and the corrected version was reposted on 9/16/2003.

References and Notes

(1) Mazurenko, Y. T.; Bakhshiev, N. G. *Opt. Spectrosc. (Transl. Opt. Spektrosk.)* **1970**, *28*, 905.
(2) Demchenko, A. P. *Ultraviolet Spectroscopy of Proteins*; Springer−Verlag: Berlin, 1987; p 183.
(3) Nemkovich, N. A.; Rubinov, A. N.; Tomin, V. I. In *Topics in Fluorescence Spectroscopy*; Lakowicz, J. R., Ed.; Plenum Press: New York, 1991; Vol. 2, p 367.
(4) Demchenko, A. P. In *Topics in Fluorescence Spectroscopy*; Lakowicz, J. R., Ed.; Plenum Press: New York, 1992; Vol. 3, p 65.
(5) Maroncelli, M.; MacInnes, J.; Fleming, G. R. *Science* **1989**, *243*, 1674.
(6) Fleming, G. R.; Cho, M. *Annu. Rev. Phys. Chem.* **1996**, *47*, 109.
(7) Stratt, R. M.; Maroncelli, M. *J. Phys. Chem.* **1996**, *100*, 12981.
(8) Nandi, N.; Bagchi, B. *J. Phys. Chem. B* **1997**, *101*, 10954.
(9) Vincent, M.; Gilles, A.-M.; Li de la Sierra, I. M.; Briozzo, P.; Barzu, O.; Gallay, J. *J. Phys. Chem. B* **2000**, *104*, 11286.
(10) Shen, X.; Knutson, J. R. *J. Phys. Chem. B* **2001**, *105*, 6260.
(11) Vivian, J. T.; Callis, P. R. *Biophys. J.* **2001**, *80*, 2093.
(12) Pal., S. K.; Peon, J.; Zewail, A. H. *Proc. Natl. Acad. Sci. U.S.A.* **2002**, *99*, 1763.
(13) Zhong, D.; Pal, S. K.; Zhang, D.; Chan, S. I.; Zewail, A. H. *Proc. Natl. Acad. Sci. U.S.A.* **2002**, *99*, 13.
(14) Peon, J.; Pal, S. K.; Zewail, A. H. *Proc. Natl. Acad. Sci. U.S.A.* **2002**, *99*, 10964.
(15) Jordanides, X. J.; Lang, M. J.; Song, X.; Fleming, G. R. *J. Phys. Chem. B* **1999**, *103*, 7995.
(16) Changenet-Barret, P.; Choma, C. T.; Gooding, E. F.; DeGrado, W. F.; Hochstrasser, R. M. *J. Phys. Chem. B* **2000**, *104*, 9322.
(17) Cohen, B. E.; McAnaney, T. B.; Park, E. S.; Jan, Y. N.; Boxer, S. G.; Jan, L. Y. *Science* **2002**, *296*, 1700.
(18) Pal, S. K.; Peon, J.; Bagchi, B.; Zewail, A. H. *J. Phys. Chem. B* **2002**, *106*, 12376.
(19) Bastiaens, P. I. H.; van Hoek, A.; van Berkel, W. J. H.; de Kok, A.; Visser, A. J. W. G. *Biochemistry* **1992**, *31*, 7061.
(20) Shcherbatska, N. V.; Bastiaens, P. I. H.; Visser, A. J. W. G.; Jonker, S. A.; Warman, J. W. *Proc. SPIE−Int. Soc. Opt. Eng.* **1992**, *1640*, 180.
(21) Bastiaens, P. I. H.; Visser, A. J. W. G. In *Fluorescence Spectroscopy. New Methods and Applications*; Wolfbeis, O. S., Ed.; Springer−Verlag: Berlin, 1993; p 49.
(22) Shcherbatska, N. V.; van Hoek, A.; Bastiaens, P. I. H.; Visser, A. J. W. G. *J. Fluoresc.* **1995**, *5*, 171.
(23) van den Berg, P. A. W.; Feenstra, K. A.; Mark, A. E.; Berendsen, H. J. C.; Visser, A. J. W. G. *J. Phys. Chem. B* **2002**, *106*, 8858.
(24) van den Berg, P. A. W.; Mulrooney, S. B.; Gobets, B.; van Stokkum, I. H. M.; van Hoek, A.; Williams, C. H., Jr.; Visser, A. J. W. G. *Protein Sci.* **2001**, *10*, 2037.
(25) Lee, J.; Matheson, I. B. C.; Müller, F.; O'Kane, D. J.; Vervoort, J.; Visser, A. J. W. G. In *Chemistry and Biochemistry of Flavoenzymes*; Müller, F., Ed.; CRC Press: Boca Raton, FL, 1991; Vol. 2, p 109.
(26) Petushkov, V. N.; Ketelaars, M.; Gibson, B. G.; Lee, J. *Biochemistry* **1996**, *35*, 12086.
(27) Petushkov, V. N.; Gibson, B. G.; Lee, J. *Biochemistry* **1996**, *35*, 8413.
(28) Kulinski, T.; Visser, A. J. W. G.; O'Kane, D. J.; Lee, J. *Biochemistry* **1987**, *26*, 540.
(29) Petushkov, V. N.; Gibson, B. G.; Lee, J. *Biochemistry* **1995**, *34*, 3300.
(30) Karatani, H.; Wilson, T.; Hastings, J. W. *Photochem. Photobiol.* **1992**, *55*, 293.
(31) Petushkov, V. N.; Gibson, B. G.; Lee, J. *Biochem. Biophys. Res. Commun.* **1995**, *211*, 774.
(32) Visser, A. J. W. G.; van Hoek, A.; Visser, N. V.; Lee, Y.; Ghisla, S. *Photochem. Photobiol.* **1997**, *65*, 570.
(33) Petushkov, V. N.; Gibson, B. G.; Visser, A. J. W. G.; Lee, J. *Methods Enzymol.* **2000**, *305*, 164.
(34) High Performance Digital Temporal Analyzer Instruction Manual. Hamamatsu Photonics Deutschland GmbH, 1995.
(35) Greene, B. J.; Farrow, R. C. *Chem. Phys. Lett.* **1983**, *98*, 273.
(36) van Stokkum, I. H. M.; Brouwer, A. M.; van Ramesdonk, H. J.; Scherer, T. *Proc. K. Ned. Akad. Wet.: Biol., Chem., Geol., Phys. Med. Sci.* **1993**, *96*, (1), 43−68.
(37) Petushkov, V. N.; Lee, J. *Eur. J. Biochem.* **1997**, *245*, 790.
(38) Reichardt, C. *Chem. Rev.* **1994**, *94*, 2319.
(39) Platenkamp, R. J.; Palmer, M. H.; Visser, A. J. W. G. *Eur. Biophys. J.* **1987,** *14*, 393.
(40) van Mourik, F.; Chergui, M.; van der Zwan, G. *J. Phys. Chem.* **2001**, *105*, 9715.
(41) van Mourik, F.; Frese, R. N.; van der Zwan, G.; Cogdell, R. J.; Van Grondelle, R. *J. Phys. Chem. B* **2003**, 107, 2156.
(42) Drössler, P.; Holzer, W.; Penzkofer, A.; Hegemann, P. *Chem. Phys.* **2002**, *282*, 429.
(43) Benigno, A. J.; Ahmed, E.; Berg, M. *J. Chem. Phys.* **1996**, *104*, 7382.
(44) Brown, R. *J. Chem. Phys.* **1995**, *102*, 9059.
(45) Sun, M.; Moore, T. A.; Song, P. S. *J. Am. Chem. Soc.* **1972**, *94*, 1730.
(46) Yagi, K.; Ohishi, N.; Nishimoto, K.; Choi, J. D.; Song, P. S. *Biochemistry* **1980**, *19*, 1553.
(47) Maroncelli, M.; Fleming, G. R. *J. Chem. Phys.* **1987**, *86*, 6221.
(48) Rosenthal, S. J.; Xie, X.; Du, M.; Fleming, G. R. *J. Chem. Phys.* **1991**, *95*, 4715.
(49) Jimenez, R.; Fleming, G. R.; Kumar, P. V.; Maroncelli, M. *Nature* **1994**, *369*, 471.
(50) Vincent, M.; Gallay, J.; Demchenko, A. P. *J. Phys. Chem.* **1995**, *99*, 14931.
(51) Morgenthaler, M. J. E.; Yoshihara, K.; Meech, S. R. *J. Chem. Soc., Faraday Trans.* **1996**, *92*, 629.
(52) Maroncelli, M.; Fleming, G. R. *J. Chem. Phys.* **1988**, *89*, 5044.

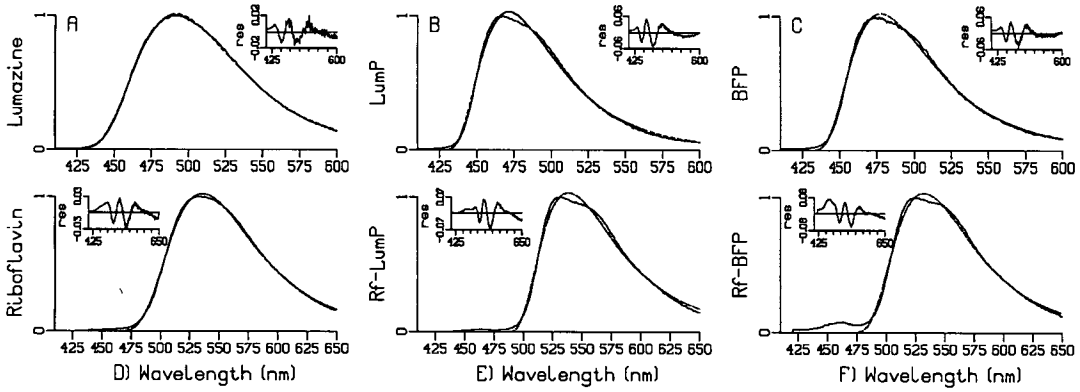

Figure S.1. Fit (dashed) of fluorescence emission spectra from Figure 1 with skewed Gaussian function (Equation 4). Free lumazine (A) and lumazine bound to antenna proteins LumP (B), and Lum-BFP (C), free riboflavin (D) and riboflavin bound to antenna proteins Rf-LumP (E) and Rf-BFP (F). Residuals are shown in insets.